DOI: 10.1002/ejic.200700530

Hybrid Organic/Inorganic Supramolecular Conductors $D_2[Au(CN)_4]$ [D = Diiodo(ethylenedichalcogeno)tetrachalcogenofulvalene], Including a New Ambient Pressure Superconductor

Tatsuro Imakubo,*[a] Takashi Shirahata,[a] Megumi Kibune,[a] and Hiroko Yoshino[a]

Keywords: Supramolecular chemistry / Conducting materials / Iodine / Superconductors / Selenium heterocycles

Five diiodo(ethylenedichalcogeno)tetrachalcogenofulvalenes, DIEDSS {2-(5,6-dihydro[1,3]diselenolo[4,5-*b*][1,4]diselenin-2-ylidene)-4,5-diiodo-1,3-dithiole}, DIET-STF {2-(4,5-diiodo-1,3-diselenol-2-ylidene)-5,6-dihydro[1,3]dithiolo[4,5-*b*][1,4]dithiine}, DIEDS-STF {2-(4,5-diiodo-1,3-diselenol-2-ylidene)-5,6-dihydro[1,4]diselenino[2,3-*d*][1,3]dithiole}, DIETSe {2-(4,5-diiodo-1,3-diselenol-2-ylidene)-5,6-dihydro[1,3]diselenolo[4,5-*b*][1,4]dithiine}, and DIEDSSe {2-(4,5-diiodo-1,3-diselenol-2-ylidene)-5,6-dihydro[1,3]diselenolo[4,5-*b*][1,4]diselenine}, have been synthesized without the use of the highly toxic reagent CSe_2, and their $Au(CN)_4$ salts have been prepared by electrochemical oxidation. Characteristic I···N iodine bonds are constructed in all crystals, and their packing motifs are classified into two groups by the difference in the space group symmetry. The salt of DIEDSS crystallizes in the monoclinic *C*2/*c* space group and a novel helical supramolecular architecture is constructed by the strong and directional I···N iodine bond. On the other hand, the rest of the four salts crystallize in the triclinic $P\bar{1}$ space group and their donor packing motifs belong to the so-called β-type. Conducting properties of the β-type salts strongly depend on the number and positions of the selenium atoms on the donor molecule. The salts based on the diselenadithiafulvalene (DSDTF) derivatives, DIET-STF and DIEDS-STF, show metal–semiconductor transition and the salt of fully selenated π-donor DIEDSSe shows stable metallic behavior down to 1.6 K. On the other hand, $(DIETSe)_2[Au(CN)_4]$ is semimetallic down to low temperature and the superconducting transition occurs at around 2 K (onset).

Introduction

The development of novel organic conductors based on tetrathiafulvalene (TTF) derivatives, which show interesting physical properties, depends not only on the design and synthesis of an independent donor molecule but also on the design of crystal structure, which is strongly related to the bulk physical properties. For designing crystal structures of organic conductors from the viewpoint of crystal engineering,[1] we have proposed the introduction of the iodine bond,[2–6] which is a special case of the halogen bond.[7] A large number of supramolecular conductors based on the iodinated TTFs have been synthesized,[8,9] and one of them, θ-$(DIETS)_2[Au(CN)_4]$ {DIETS = 2-(4,5-diiodo-1,3-dithiol-2-ylidene)-5,6-dihydro[1,3]diselenolo[4,5-*b*][1,4]dithiine}, shows superconductivity under uniaxial strain applied along the I···N iodine bond.[3c] It is well known that replacement of the sulfur atom in the TTF skeleton by the selenium atom is an effective method of increasing electrical conductivity and the development of organic superconductors.[10] Recently, we have reported a new CSe_2-free synthesis of 1,3-diselenole-2-thione, which may be a good alternative to 1,3-diselenole-2-selone, together with its applications to the synthesis of 4,5-diiodo-1,3-diselenole-2-one[5] and 4,5-alkylenedichalcogeno-1,3-diselenole-2-ones.[6] Cross-coupling reactions using these 1,3-diselenole-2-ones provide a number of selenium analogues of DIETS, i.e., DIEDSS {2-(5,6-dihydro[1,3]diselenolo[4,5-*b*][1,4]diselenin-2-ylidene)-4,5-diiodo-1,3-dithiole}, DIET-STF {2-(4,5-diiodo-1,3-diselenol-2-ylidene)-5,6-dihydro-[1,3]dithiolo[4,5-*b*][1,4]dithiine}, DIEDS-STF {2-(4,5-diiodo-1,3-diselenol-2-ylidene)-5,6-dihydro[1,4]diselenino-[2,3-*d*][1,3]dithiole}, DIETSe {2-(4,5-diiodo-1,3-diselenol-2-

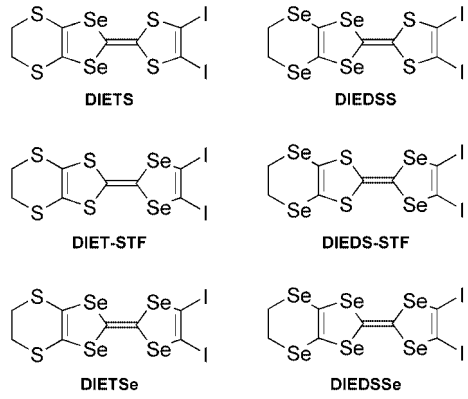

Figure 1. Molecular structure of iodinated TTFs.

[a] Imakubo Initiative Research Unit, RIKEN,
2-1 Hirosawa, Wako, Saitama 351-0198, Japan
E-mail: imakubo@riken.jp

ylidene)-5,6-dihydro[1,3]diselenolo[4,5-*b*][1,4]dithiine}, and DIEDSSe {2-(4,5-diiodo-1,3-diselenol-2-ylidene)-5,6-dihydro[1,3]diselenolo[4,5-*b*][1,4]diselenine}, and these organic π-donors are suitable candidates for the exploration of novel supramolecular organic conductors and superconductors. In this article, we report on the synthesis, crystal structure, and physical properties of novel supramolecular organic conductors $D_2[Au(CN)_4]$ (D = organic π-donors mentioned above, see Figure 1) together with the details of the synthesis of the neutral π-donors.

Results and Discussion

Donor Synthesis

The first synthesis of 4,5-ethylenediseleno-1,3-diselenole-2-selone (**1a**) was accomplished by the electrochemical reduction of CSe_2.[11] However, the reduction process of CSe_2 is dangerous and not ideal from the viewpoint of a safe laboratory environment. A modified synthesis of **1a** using bis(selenocyanato)ethane as the electrophile was reported by Otsubo et al.,[12] however CSe_2 is still indispensable for the synthesis of the starting material 1,3-diselenole-2-selone.[13] Recently, we have reported a CSe_2-free synthesis of 1,3-diselenole-2-thione, which seems to be a good starting material for the synthesis of the thione **1b**. At first, we applied the same reaction conditions for the synthesis of **1a** from 1,3-diselenole-2-selone to the synthesis of **1b** from 1,3-diselenole-2-thione. However, the main product of the reaction was the 1,3-thiaselenole-2-selone **2** (20%) and the desired thione **1b** was obtained in only 3% yield. To avoid the unfavorable transformation of 1,3-diselenole-2-thione to 1,3-thiaselenole-2-selone, we changed the reaction sequence as well as the iodination of 1,3-diselenole-2-thione,[5] that is, LDA was added last to a solution of 1,3-diselenole-2-thione and 1,2-bis(selenocyanato)ethane. This inverted sequence afforded **1b** without a selenium–sulfur exchange side reaction in a yield of under 5%. The low yield of **1b** was improved under the diluted conditions, which avoided the polymerization of the intermediate anions. In the optimized reaction conditions, the yield of **1b** exceeded 20%, and about 40% of the starting material 1,3-diselenole-2-thione, which can be recycled for the same reaction, was recovered. The thione **1b** was easily converted into the corresponding ketone **1c** (89%) by the conventional $Hg(OAc)_2/CHCl_3$ method. Phosphite-mediated cross-coupling reactions between the 1,3-dichalcogenole units in Scheme 1 gave diiodo(ethylenedichalcogeno)tetrachalcogenofulvalenes, DIEDSS, DIET-STF, DIEDS-STF, DIETSe,[4] and DIEDSSe. The results of the cross-coupling reactions and the redox potentials of a series of DIETS analogues are summarized in Table 1. These π-donors show two reversible waves and their donor abilities mainly depend on the inner fulvalene skeleton. The diselenadithiafulvalene (DSDTF) derivatives, DIETS, DIEDSS, DIET-STF, and DIEDS-STF, show lower $E_1^{1/2}$ than tetraselenafulvalene (TSeF) derivatives, DIETSe and DIEDSSe. On the other hand, the smaller ΔE values of TSeFs suggest the smaller on-site Coulombic repulsion thanks to the introduction of larger selenium atoms, which extend the highest occupied molecular orbital (HOMO).

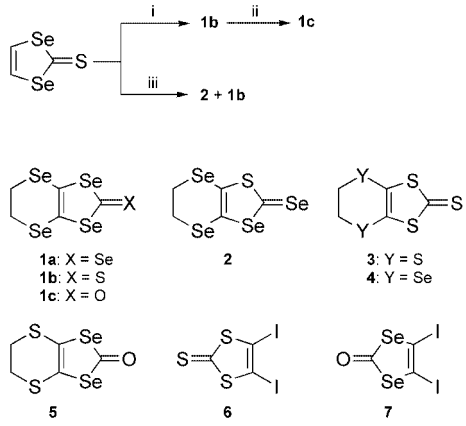

Scheme 1. Reagents and conditions: (i) 1,2-bis(selenocyanato)ethane (1.2 equiv.), then LDA (2.5 equiv.), –78 °C; (ii) $Hg(OAc)_2$, $AcOH/CHCl_3$; (iii) LDA (2.2 equiv.) then 1,2-bis(selenocyanato)ethane (1.6 equiv.), –78 °C.

Preparation of the $Au(CN)_4$ Salts

Single crystals of the $Au(CN)_4$ salts were prepared by the galvanostatic oxidation of a CH_2Cl_2 solution containing DIEDSS, DIET-STF, DIEDS-STF, DIETSe, or DIEDSSe and tetrabutylammonium tetracyanoaurate as the supporting electrolyte. The five cation radical salts, $(DIEDSS)_2[Au(CN)_4]$ (**8**), $(DIET\text{-}STF)_2[Au(CN)_4]$ (**9**), $(DIEDS\text{-}STF)_2[Au(CN)_4]$ (**10**), $(DIETSe)_2[Au(CN)_4]$ (**11**), and $(DIEDSSe)_2[Au(CN)_4]$ (**12**), are classified into two groups according to the difference in their space group symmetry. The salt **8**

Table 1. Results of the cross-coupling reactions and cyclic voltammetry data[a] for diiodo(ethylenedichalcogeno)tetrachalcogenofulvalenes.

Donor	Materials	Solvent	% Yield[b]	Color	$E_1^{1/2}$ [V]	$E_2^{1/2}$ [V]	ΔE (=$E_2^{1/2} - E_1^{1/2}$)
TTF					–0.10	0.32	0.42
DIETS[c]	**5** + **6**	toluene	74	orange-red	0.22	0.49	0.27
DIEDSS	**1c** + **6**	toluene	48	orange-brown	0.24	0.51	0.27
DIET-STF	**3** + **7**	benzene	76	purplish-brown	0.21	0.49	0.28
DIEDS-STF	**4** + **7**	benzene	71	orange-brown	0.19	0.47	0.28
DIETSe[d]	**5** + **7**	toluene	28	dark green	0.31	0.55	0.24
DIEDSSe	**1b** + **7**	toluene	21	orange	0.29	0.52	0.23

[a] vs. Cp_2Fe–Cp_2Fe^+ couple, in PhCN with 0.1 M nBu_4NBF_4, glassy carbon working electrode, 100 mV s^{-1}, room temp. [b] Isolated yields. [c] From ref.[3]. [d] From ref.[4].

Table 2. Crystal data for $D_2[Au(CN)_4]$.[a]

	8	**9**	**10**	**11**	**12**
Donor	DIEDSS	DIET-STF	DIEDS-STF	DIETSe	DIEDSSe
Empirical formula	$C_{20}H_8AuI_4N_4S_4Se_8$	$C_{20}H_8AuI_4N_4S_8Se_4$	$C_{20}H_8AuI_4N_4S_4Se_8$	$C_{20}H_8AuI_4N_4S_4Se_8$	$C_{20}H_8AuI_4N_4Se_{12}$
Formula mass	1768.79	1581.19	1768.79	1768.79	1956.39
Crystal system	monoclinic	triclinic	triclinic	triclinic	triclinic
Space group	*C*2/*c* (#15)	$P\bar{1}$ (#2)	$P\bar{1}$ (#2)	$P\bar{1}$ (#2)	$P\bar{1}$ (#2)
a [Å]	35.567(11)	7.4187(15)	7.4317(17)	7.3866(17)	7.4097(18)
b [Å]	4.8049(15)	8.0234(16)	8.1410(19)	8.0530(19)	8.153(2)
c [Å]	23.150(7)	16.212(3)	16.304(4)	16.413(4)	16.498(4)
α [°]	90	79.077(4)	78.999(5)	79.272(5)	79.021(5)
β [°]	112.379(6)	78.369(4)	78.441(4)	78.358(5)	78.479(4)
γ [°]	90	68.194(4)	69.144(4)	68.177(4)	68.911(5)
V [Å^3]	3658(2)	870.5(3)	895.4(4)	881.0(4)	903.5(4)
Z	4	1	1	1	1
D_{calcd} [g cm^{-3}]	3.212	3.016	3.280	3.334	3.596
μ(Mo-K_α) [mm^{-1}]	15.608	12.456	15.942	16.202	19.597
Collected reflections	12382	6485	6686	6601	6737
Independent reflections	4649	4225	4344	4299	4418
R_{int}	0.1253	0.0525	0.0662	0.0647	0.0728
R_1, wR_2 [$I > 2\sigma(I)$]	0.0582, 0.1136	0.0338, 0.0882	0.0369, 0.0956	0.0477, 0.1244	0.0422, 0.1042
R_1, wR_2 (all data)	0.1574, 0.1363	0.0384, 0.0988	0.0436, 0.0976	0.0574, 0.1344	0.0525, 0.1164
Gof	0.869	1.034	0.979	0.987	0.963
$d_{I\cdots N}$ [Å][b]	2.99(2), 3.28(1)	2.856(9)	2.86(1)	2.83(1)	2.86(1)

[a] Measured at 293 K. [b] Sum of the van der Waals radii: I···N = 3.53 Å.[14]

based on DIEDSS, which contains a 4,5-diiodo-1,3-dithiole unit, crystallizes in the monoclinic *C*2/*c* space group, whereas the salts **9**–**12** based on the π-donors containing the 4,5-diiodo-1,3-diselenole unit crystallize in the triclinic $P\bar{1}$ space group (Table 2).

Crystal Structure

The salt **8** crystallizes in the monoclinic *C*2/*c* space group (Table 2) and its crystal structure is shown in Figure 2. The donor/anion ratio is 2:1 and one crystallographically independent donor molecule stacks uniformly in a head-to-head manner along the crystallographic *b* axis. The gold atom of the $Au(CN)_4$ anion is located on the twofold axis and the almost planar $Au(CN)_4$ anion also stacks along the crystallographic *b* axis. The molecular packing motif of **8** basically resembles that of θ-$(DIETS)_2[Au(CN)_4]$,[3c] which is also based on the π-donor containing the 4,5-diiodo-1,3-dithiole unit. However, the donor columns A and B (A′ and B′) solid-cross along the side-by-side direction (Figure 3a). On the other hand, the donor columns A and A′ (B and B′) are parallel and they correspond to a part of the so-called β"-type structure, as shown in Figure 3b. Differences in the crystal structure between θ-$(DIETS)_2[Au(CN)_4]$ and **8** originate from the external form of the donor molecule. The steric hindrance between the donor molecules along the side-by-side direction in the crystal of **8** is larger than that in θ-$(DIETS)_2[Au(CN)_4]$ because DIEDSS contains a larger ethylenediseleno group than DIETS, which contains a smaller ethylenedithio group. A solid-crossing molecular arrangement of the DIEDSS molecule seems favorable for

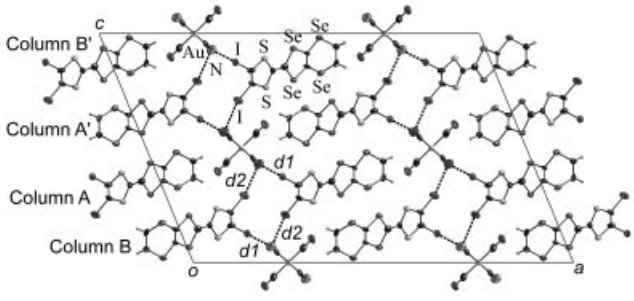

Figure 2. Crystal structure of **8** viewed along the crystallographic *b* axis. The dotted lines indicate I···N iodine bonds [*d*1 = 2.99(2), *d*2 = 3.28(1) Å].

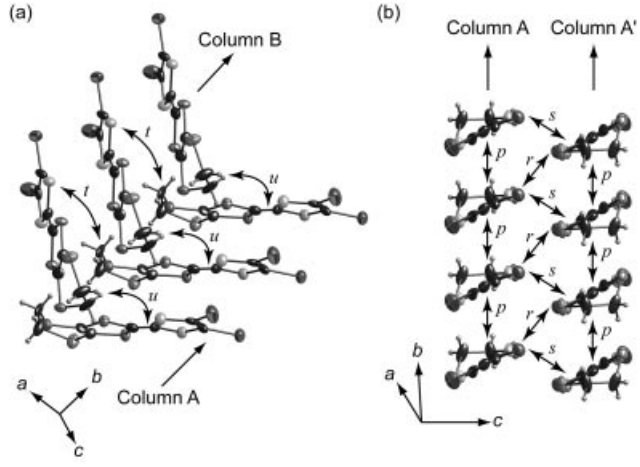

Figure 3. Molecular arrangement of the donor molecule of **8**: (a) solid-crossing arrangement for Column A and B viewed along the side-by-side direction of the donor molecule of Column A; (b) β"-type arrangement for Column A and A′ viewed along the long molecular axis of DIEDSS. The calculated overlap integrals ($\times 10^{-3}$) are *p* = –1.49, *r* = 1.41, *s* = –11.34, *t* = 0.17, *u* = 2.55.

avoiding steric repulsion between the larger ethylenediseleno groups.

As well as the other organic conductors based on iodinated TTFs, strong I···N iodine bonds are observed in **8**. The I···N distances are $d1$ = 2.99(2) Å and $d2$ = 3.28(1) Å and they are 7–15% shorter than the sum of the van der Waals radii (3.53 Å).[14] Along the crystallographic b axis, there is a helix of ···I–C=C–I···N···I–C=C–I···N··· and the helices are connected along the c axis through the $Au(CN)_4$ anions, as shown in Figure 4.

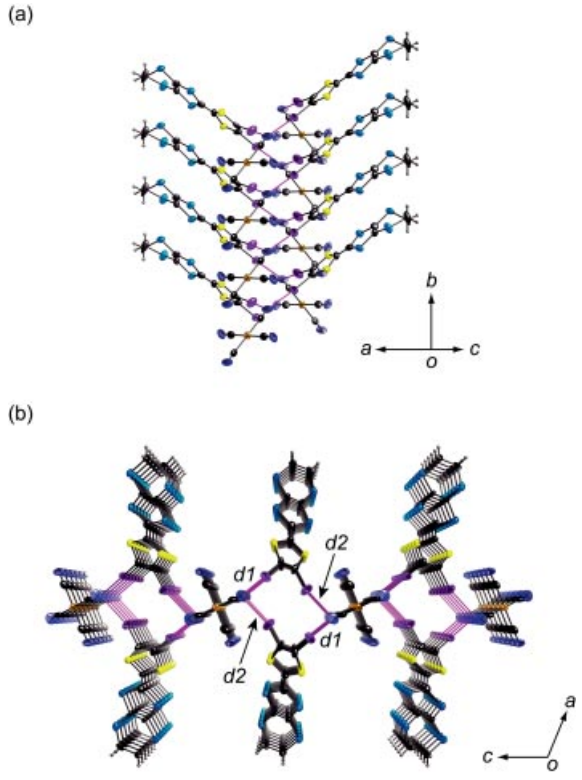

Figure 4. Helical supramolecular architecture in **8** constructed by the iodine bond (a) viewed along the $a + c$ axis; (b) projection onto the ac plane. The pink lines indicate I···N iodine bonds [$d1$ = 2.99(2), $d2$ = 3.28(1) Å].

On the other hand, the $Au(CN)_4$ salts **9**–**12** based on the π-donors containing the 4,5-diiodo-1,3-diselenole unit, DIET-STF, DIEDS-STF, DIETSe, and DIEDSSe, are isostructural and crystallize in the triclinic $P\bar{1}$ space group (Table 2). The crystal structure of **11** is shown in Figure 5 as a representative of the isomorphic salts **9**–**12**. The unit cell contains two donor molecules and one $Au(CN)_4$ anion, and the donor/anion ratio is 2:1. The donor molecules stack in a head-to-tail manner along the crystallographic b axis and the so-called β-type structure is constructed within the ab plane. Short I···N iodine bonds ($d3$ = 2.83–2.86 Å, see the last row of Table 2), which are 19–20% shorter than the sum of the van der Waals radii, are observed.

Three types of iodine bonds, $d1$ and $d2$ for **8**, and $d3$ for **11** as the representative of the β-type salts **9**–**12**, are depicted in Figure 6 together with the lowest unoccupied molecular orbitals (LUMOs) of DIEDSS and DIETSe. In the

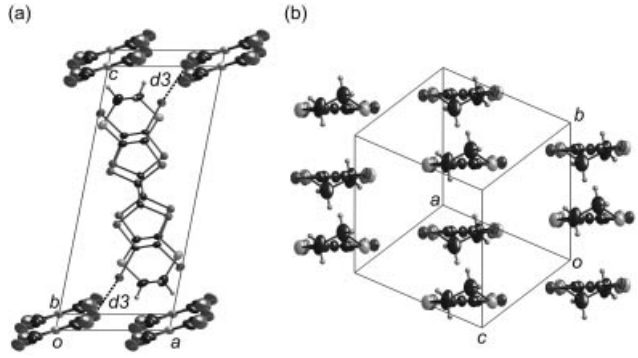

Figure 5. Crystal structure of **11**. (a) A projection onto the ac plane. The dotted lines indicate I···N iodine bonds [$d3$ = 2.83(1) Å] shorter than the sum of the van der Waals radii. (b) Molecular arrangement of the donor molecule viewed along the long molecular axis of DIETSe.

case of $d1$, the donor molecule and the $Au(CN)_4$ anion are almost parallel, which is similar to the situation in θ-$(DIETS)_2[Au(CN)]_4$,[3c] and nearly orthogonal arrangements of the donor molecule and the $Au(CN)_4$ anion are observed in the cases of $d2$ and $d3$. From the viewpoint of the relationship between the molecular structure and the geometrical conformation of the iodine bond, the chalcogen element of the dichalcogenole ring on the iodine-bonded side of the molecule seems essential. A "parallel" arrangement like $d1$ is observed only in the salts based on the donor molecules containing the 4,5-diiodo-1,3-dithiole unit, that is, **8** and θ-$(DIETS)_2[Au(CN)]_4$. On the other hand, an "orthogonal" arrangement is preferred in the salts **9**–**12**, which are based on the donor molecules containing the 4,5-diiodo-1,3-diselenole unit. According to the calculated coefficients of the LUMOs on the 4,5-diiodo-1,3-dichalcogenole

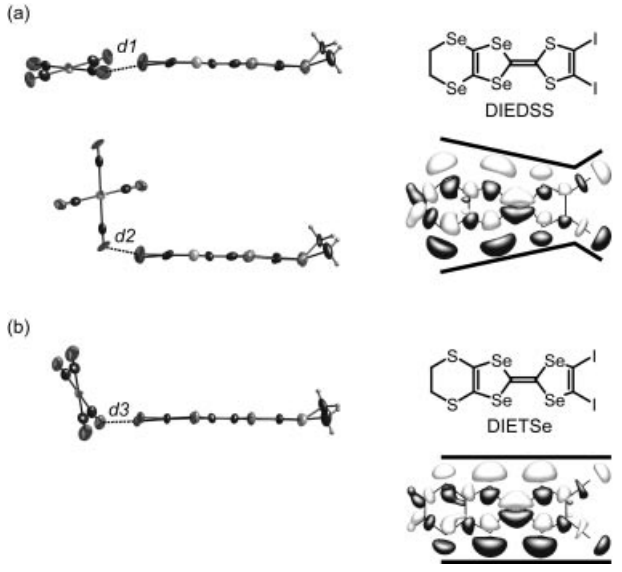

Figure 6. Three types of iodine bond, $d1$, $d2$, and $d3$, and LUMO of DIEDSS and DIETSe calculated by the MNDO–PM3 method;[15] (a) $d1$ and $d2$ for the salt **8** and LUMO of DIEDSS; (b) $d3$ for the salt **11** and LUMO of DIETSe. The solid lines are a guide for the eyes.

unit, the coefficients of the LUMO on the sulfur atoms of the 4,5-diiodo-1,3-dithiole unit are clearly smaller than those of the selenium atoms on the 4,5-diiodo-1,3-diselenole unit. Therefore, the differences in the geometrical conformation of the iodine bonds seem to be related not only to the external form of the donor molecules but also to the spatial extent of the frontier molecular orbitals around the 4,5-diiodo-1,3-dichalcogenole unit. In the salt **8**, there are two types of iodine bond, that is, "parallel" *d*1 and "orthogonal" *d*2, and the coexistence of these two types of iodine bond is essential to the helical supramolecular architecture.

Band Calculation

Intermolecular overlap integrals for the salt **8** calculated by the extended Hückel method[16] are shown in Figure 3. The overlap integral *s* is considerably larger than the other overlap integrals *p*, *r*, *t*, and *u*, and the donor molecules are strongly dimerized along the side-by-side direction. The calculated band dispersion and the Fermi surfaces for **8** based on the tight-binding approximation using these overlap integrals are shown in Figure 7. There are four bands built from the HOMOs of the four donor molecules within the primitive cell [$a_p = (a + b)/2$, $b_p = b$, $c_p = c$] and they are separated by a gap in the upper and lower bands because of the strong dimerization mentioned above. Although the calculated Fermi surfaces are warped and quasi-one-dimensional, the calculated bandwidth of the upper band (ca. 0.08 eV) is much smaller than those of the usual organic conductors based on TTFs, and the strong electron correlation must be disadvantageous to achieving the metallic conductivity.

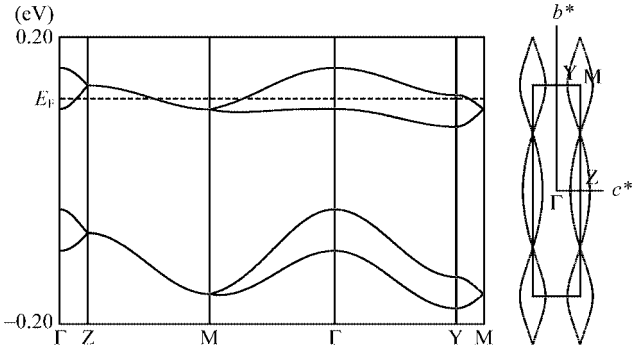

Figure 7. Calculated electronic band dispersion (left) and Fermi surfaces (right) for **8**.

Figure 8 shows a schematic view of the molecular arrangement within the donor layer for the β-type salts **9**–**12**, and the calculated overlap integrals are listed in Table 3. Differences in the intrastack overlap integrals between *p* and *q* are small enough to be regarded as a regular column structure. The interstack overlap integrals *r*, *s*, and *t* are about 1/7–1/19 of the intrastack overlap integrals *p* and *q*, and the quasi-one-dimensional character of the electronic band structure is suggested. The enhancement of the overlap integrals for **9** and **10** compared with those of **11** and **12** is accomplished by the replacement of sulfur atoms on the DSDTF skeleton with selenium atoms. On the other hand, the calculated overlap integrals of the side-by-side direction *s* and *t* for **9** based on the ethylenedithio derivative are slightly larger than those of **10** based on the ethylenediseleno derivative. There is a similar relationship between **11** and **12**, indicating that the overlap integrals *s* and *t* for the salts **10** and **12** are reduced by the steric repulsion of the larger ethylenediseleno group. The calculated band dispersion and the Fermi surfaces for **11** are shown in Figure 9 as a representative of the β-type salts **9**–**12**. There are two

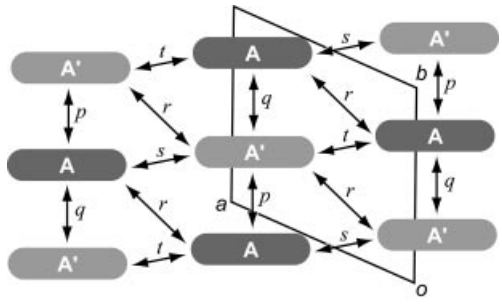

Figure 8. Schematic view of the donor layer for **9**–**12**.

Table 3. Calculated overlap integrals for **9**–**12** ($\times 10^{-3}$).[a]

	9	10	11	12
p	–12.63	–13.42	–18.36	–16.61
q	–14.82	–14.48	–18.55	–17.17
r	–0.77	–0.82	–1.03	–1.07
s	1.71	1.52	2.20	1.78
t	1.67	1.15	2.01	1.51

[a] See Figure 8 for the symbols of the overlap integrals.

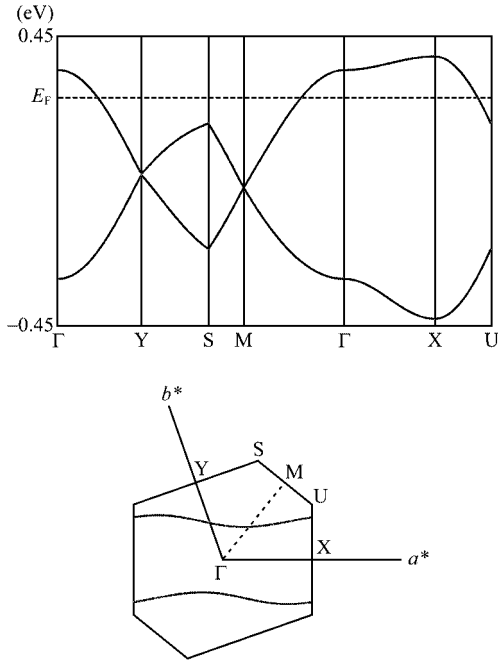

Figure 9. Calculated electronic band dispersion (top) and Fermi surfaces (bottom) for **11**.

bands built from the HOMOs of the two donor molecules within the unit cell, and there is no gap between the upper and lower bands. This is consistent with the regular column structure of the donor molecule. The calculated Fermi surfaces are quasi-one-dimensional along the *b* axis, which is the stacking direction of the donor molecule. The Fermi surfaces and electronic band dispersions for the salts **9**–**12** are almost the same except for the calculated bandwidth, and thanks to the TSeF skeleton, the bandwidths of **11** and **12** (about 0.7–0.8 eV) are larger than those of **9** and **10** (about 0.6 eV), and **11** and **12** are expected to have a stable metallic nature.

Conducting Property

The single crystal of the salt **8** is a semiconductor with a small activation energy (E_a = 98 meV) and the room temperature resistivity is 2.3 Ω cm. There are a few examples of helical architecture in organic crystals based on TTFs, however they are insulators.[17] To the best of our knowledge, the salt **8** is the first example of a highly conductive crystal that has helical architecture based on TTFs.

The room-temperature resistivities of the single crystals of the β-type salts **9**–**12** are 1.8×10^{-2}, 1.7×10^{-2}, 1.4×10^{-2}, and 1.6×10^{-2} Ω cm, respectively. Figure 10 shows the temperature dependence of the resistivities for **9**–**12**. The conducting behavior of **9**–**12** strongly depends on the number and the positions of the selenium atoms on the donor molecule. The salts **9** and **10** based on the DSDTF derivatives show metal–semiconductor transition at 85 K for **9** and at 155 K for **10**. The metallic state of **9** based on the ethylenedithio derivative DIET-STF is more stable than that of **10** based on the ethylenediseleno derivative DIEDS-STF. It is consistent with the band calculation mentioned above, that is, the ethylenediseleno group reduces the overlap integrals of the side-by-side direction because of the steric repulsion and lowers the dimensionality of the electronic band structure.

The salt **12** based on the fully selenated π-donor DIEDSSe shows metallic behavior down to 1.6 K and the stable metallic nature is derived from the full replacement of the sulfur atoms in the diiodo(ethylenedichalcogeno)tetrachalcogenofulvalene with selenium atoms. On the other hand, the salt **11** shows semimetallic behavior down to 2 K and then a distinct resistivity drop, which is characteristic of the onset of superconductivity, was observed for several crystals (Figure 10b). Complete superconductivity with zero resistivity has not been confirmed because of its low transition temperature and the limit of the measurement apparatus. In spite of the identical crystal morphology among samples 1–4, there is a sample dependency of the onset temperature of the superconducting transition (T_c): 1.8 K for samples 1–3 and 2.1 K for sample 4. The crystals of **11** are fragile and the sample dependence of the T_c may be affected by cracks in the crystals. Resistivity jumps were observed in all samples at higher temperatures, that is, at around 80 K for sample 1, 60 K for sample 2, 90 K for sample 3, and 100 K for sample 4. Samples 1 and 2 were harvested from the same crystallization cell (Batch A), and samples 3 and 4 were obtained from a different experiment (Batches B and C, respectively). The conditions of electrochemical oxidation for Batches A and B are almost the same and no clear relationship was observed between the conditions of crystal preparation and the T_c of superconductivity.

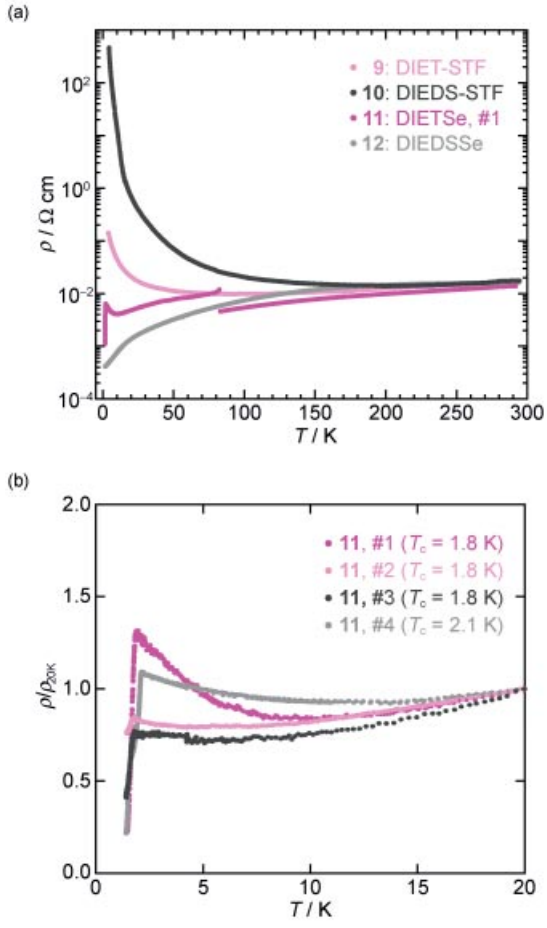

Figure 10. (a) Temperature dependence of the resistivities for **9** (light magenta), **10** (dark grey), **11** (sample 1, dark magenta), and **12** (light grey). (b) Normalized resistivities for **11** in the low-temperature region (samples 1: dark magenta, 2: light magenta, 3: dark grey, 4: light grey).

Figure 11 shows the temperature dependence of the DC magnetizations for the crystals of **11** obtained from Batches A, B, and C, which include samples 1 and 2, 3, and 4, respectively. The onset of the diamagnetic transition occurred at 1.8 K for Batches A and B, and at 1.9 K for Batch C. The higher transition temperature of Batch C is consistent with the resistivity measurement for sample 4. Owing to the very low applied field of 10 Oe and the low T_c, absolute values of magnetic susceptibility (χ) and the volume fraction of superconductivity cannot be calculated, however the appearance of the diamagnetic transition is clear evidence for the superconducting transition of the salt **11**. The inset of Figure 11 shows the temperature dependence of the magnetic susceptibility for **11** under an applied field of 50 kOe. Magnetic susceptibility χ is almost independent of

temperature above T_c and shows Pauli paramagnetism. It is also confirmed that the jumps of resistivity at 60–100 K are not intrinsic but result from the fragility of the crystals.

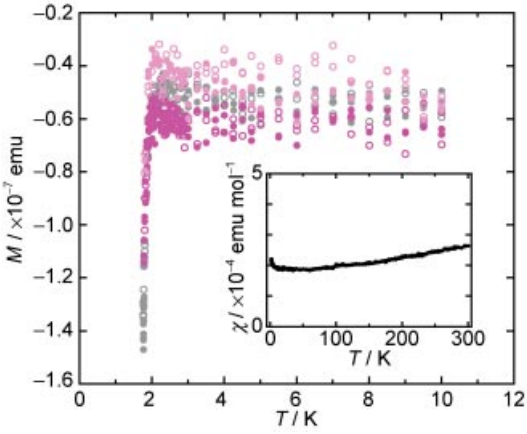

Figure 11. Temperature dependence of ZFC (filled circles) and FC (open circles) DC magnetizations for **11** (raw data). The dark magenta circles are data on Batch A including samples 1 and 2 in Figure 10b, the light magenta circles are data on Batch B including sample 3 in Figure 10b, and the light grey circles are data on Batch C including sample 4 in Figure 10b under an applied field of 10 Oe. The inset shows the temperature dependence of the magnetic susceptibility for **11** under an applied field of 50 kOe.

Conclusions

We have synthesized five selenium-rich π-donors, DIEDSS, DIET-STF, DIEDS-STF, DIETSe, and DIEDSSe, without the use of CSe_2, and the crystal structure and electronic properties of their $Au(CN)_4$ salts were systematically investigated. The chalcogen element of the 4,5-diiodo-1,3-dichalcogenole unit of the donor molecule is essential to the packing motif of the crystals. The $Au(CN)_4$ salt of DIEDSS, which contains the 4,5-diiodo-1,3-dithiole unit, includes a novel helical architecture tailored by two types of the characteristic iodine bond. This salt is also the first example of a highly conductive crystal that has helical architecture based on TTFs. On the other hand, the crystal structure of the $Au(CN)_4$ salts based on donor molecules containing the 4,5-diiodo-1,3-diselenole unit, DIET-STF, DIEDS-STF, DIETSe, and DIEDSSe, is of the so-called β-type. Their conducting behavior strongly depends on the number and positions of the selenium atoms on the donor molecule and varies from semiconductor to superconductor. Among the four β-type crystals, the salt of DIETSe shows superconducting transition at around 2 K (onset), and this is the first ambient pressure organic superconductor based on halogenated TTFs. These results indicate that a combination of supramolecular architecture based on the iodine bond and enhancement of electrical conductivity by sulfur–selenium replacement is a promising method for the stepwise development of new organic superconductors.

Experimental Section

General: All chemicals and solvents were of reagent grade. All reactions were conducted under argon except for the oxidation reactions using $Hg(OAc)_2$. Dehydrated THF and 4,5-ethylenedithio-1,3-dithiole-2-thione (**3**) were purchased from Kanto Chemical Co., Inc. and Tokyo Chemical Industry Co., Ltd., respectively, and used without further purification. A THF solution of LDA was prepared from diisopropylamine with an *n*-hexane solution of *n*BuLi prior to use. Column chromatography was carried out with silica gel (Kanto Chemical Co., Inc., 100–210 μm). Preparative gel permeation chromatography (GPC) was performed on a Japan Analytical Industry Co., Ltd. LC-908W equipped with a JAI-GEL 1H, 2H column assembly. ^{1}H NMR spectra were recorded with a JEOL JNM-Excalibur 270 spectrometer. The chemical shifts are given in δ ppm, downfield from internal Me_4Si. Mass spectra were taken in the EI mode with ionization energy of 70 eV, using a Shimadzu QP-5050A quadrupole mass spectrometer. The melting points were determined from the TG-DTA analyses using a SII EXSTAR6000 analyzer. IR spectra were recorded with a Shimadzu FTIR-8100M spectrometer with a PIKE MIRacle diamond ATR. Elemental analyses were performed at the Advanced Development & Supporting Center, RIKEN. Cyclic voltammetry measurements were performed under argon using a BAS ALS-model610A analyzer.

4,5-Ethylenediseleno-1,3-diselenole-2-thione (1b): A THF solution of LDA (0.40 M, 2.8 mL, 1.1 mmol) was slowly added to a mixture of 1,3-diselenole-2-thione[5] (102 mg, 0.45 mmol) and 1,2-bis(selenocyanato)ethane[13] (129 mg, 0.54 mmol) in dehydrated THF (100 mL) at –78 °C for a period of 5 min. The reaction mixture was stirred for 1 h at –78 °C, then quenched by addition of H_2O/THF (1 mL, v:v = 1:1) and warmed to room temperature. After stirring overnight at room temperature, the resulting reddish brown solution was poured into dichloromethane (100 mL), washed with water (100 mL, three times), dried with $MgSO_4$, and then concentrated under reduced pressure. The residue was subjected to silica-gel column chromatography. The first yellow fraction eluted with CS_2/*n*-hexane (4:1) was **1b** (39 mg, 21%) as an ocher powder upon concentration, and the second yellow band gave the recovered 1,3-diselenole-2-thione (44 mg, 43%) as a yellow-brown solid upon concentration. Analytically pure **1b** was obtained by further purification by preparative GPC. M.p. 130 °C. MS (EI, 70 eV): *m*/*z* = 414 [M^+ for $C_5H_4S^{78}Se^{80}Se_3$], 370 [M^+ – C=S]. ^{1}H NMR (270 MHz, $CDCl_3$): δ = 3.47 (s, 4 H) ppm. IR (neat): $\tilde{\nu}$ = 1001 (s), 1024 (s), 1096 (w), 1130 (w), 1217 (w), 1262 (m), 1395 (m), 1416 (w), 1458 (w), 1509 (w), 1522 (w) cm^{-1}. $C_5H_4SSe_4$ (411.99): calcd. C 14.58, H 0.98; found C 14.34, H 0.82.

4,5-Ethylenediseleno-1,3-diselenol-2-one (1c): Acetic acid (5 mL) was added to a suspension of **1b** (209 mg, 0.51 mmol) and $Hg(OAc)_2$ (339 mg, 1.06 mmol) in chloroform (25 mL), and the resulting suspension was then stirred for 5 h at room temperature. The resulting yellow-white suspension was filtered through Celite and washed with dichloromethane. The combined filtrate was washed with aqueous $NaHCO_3$ (100 mL, three times) and water (100 mL, twice), dried with $MgSO_4$, and then concentrated under reduced pressure. The residue was subjected to silica-gel column chromatography eluted with dichloromethane and pure **1c** was obtained as a cream powder (179 mg, 89%). The analytical data are identical to the reported data.[12]

4,5-Ethylenediseleno-1,3-thiaselenol-2-selone (2): A THF solution of LDA (0.75 M, 1.2 mL, 0.92 mmol) was added to a solution of 1,3-diselenole-2-thione[5] (96 mg, 0.42 mmol) in THF (100 mL) at –78 °C, and the resulting solution was stirred for 1 h at the same temperature. 1,2-Bis(selenocyanato)ethane[13] (157 mg, 0.66 mmol)

was added to this reaction mixture in one portion. After 15 min, the mixture was warmed to room temperature, then the resulting dark red solution was poured into dichloromethane (200 mL), washed with water (100 mL, four times), dried with $MgSO_4$, and then concentrated under reduced pressure. The residue was subjected to silica-gel column chromatography. The first yellow fraction eluted with CS_2 was **1b** (6 mg, 3%) as an ocher powder upon concentration, and the second orange band eluted with CS_2 gave **2** (35 mg, 20%) as a purplish-brown crystal upon concentration. M.p. 170 °C (dec.). MS (EI, 70 eV): m/z = 414 [M^+ for $C_5H_4S^{78}Se^{80}Se_3$]. ^1H NMR (270 MHz, $CDCl_3$): δ = 3.44 (m, 2 H), 3.45 (m, 2 H) ppm. IR (neat): $\tilde{\nu}$ = 922 (s), 939 (m), 1021 (w), 1086 (w), 1136 (w), 1223 (w), 1258 (m), 1402 (m), 1453 (m) cm^{-1}. $C_5H_4SSe_4$ (411.99): calcd. C 14.58, H 0.98; found C 14.59, H 0.91.

2-(5,6-Dihydro[1,3]diselenolo[4,5-*b*][1,4]diselenin-2-ylidene)-4,5-diiodo-1,3-dithiole (DIEDSS): $P(OEt)_3$ (2.8 mL) was added dropwise over a period of 10 min to a refluxing solution of **6**[3b,8a] (154 mg, 0.40 mmol) and **1c** (128 mg, 0.26 mmol) in toluene (20 mL), followed by stirring under reflux for 30 min. After cooling to room temperature, the solution was evaporated under reduced pressure to eliminate the solvent and excess phosphite. The residue was subjected to silica-gel column chromatography. The second violet fraction eluted with CS_2 was collected, and DIEDSS was obtained as orange-brown crystals (114 mg, 48%). M.p. 157 °C (dec.). MS (EI, 70 eV): m/z = 736 [M^+ for $C_8H_4I_2S_2{}^{78}Se^{80}Se_3$]. ^1H NMR (270 MHz, $CDCl_3$): δ = 3.37 (s, 4 H) ppm. IR (neat): $\tilde{\nu}$ = 1092 (s), 1136 (m), 1219 (w), 1262 (s), 1399 (m), 1416 (m), 1480 (w), 1507 (w) cm^{-1}. $C_8H_4I_2S_2Se_4$ (733.90): calcd. C 13.09, H 0.55; found C 13.14, H 0.53.

2-(4,5-Diiodo-1,3-diselenol-2-ylidene)-5,6-dihydro[1,3]dithiolo[4,5-*b*]-[1,4]dithiine (DIET-STF): $P(OEt)_3$ (3.7 mL) was added dropwise over a period of 5 min to a refluxing solution of **7**[5] (100 mg, 0.22 mmol) and **3** (58 mg, 0.26 mmol) in benzene (20 mL), followed by stirring under reflux for 1.5 h. The same procedure as for DIEDSS was adopted for the separation of the products. Evaporation of the second red-orange fraction afforded purplish-brown crystals of DIET-STF (104 mg, 76%). M.p. 175 °C (dec.). MS (EI, 70 eV): m/z = 642 [M^+ for $C_8H_4I_2S_4{}^{80}Se_2$]. ^1H NMR (270 MHz, $CDCl_3$): δ = 3.30 (s, 4 H) ppm. IR (neat): $\tilde{\nu}$ = 1125 (s), 1173 (m), 1258 (m), 1283 (s), 1404 (m), 1499 (m), 1509 (m) cm^{-1}. $C_8H_4I_2S_4Se_2$ (640.11): calcd. C 15.01, H 0.63; found C 14.96, H 0.53.

2-(4,5-Diiodo-1,3-diselenol-2-ylidene)-5,6-dihydro[1,4]diselenino[2,3-*d*]-[1,3]dithiole (DIEDS-STF): $P(OEt)_3$ (3.7 mL) was added dropwise over a period of 3 min to a refluxing solution of **7**[5] (100 mg, 0.22 mmol) and **4**[18] (82 mg, 0.26 mmol) in benzene (20 mL), followed by stirring under reflux for 3 h. The same procedure as for DIEDSS was adopted for the separation of the products. Evaporation of the second red-orange fraction afforded orange-brown crystals of DIEDS-STF (112 mg, 71%). M.p. 154 °C (dec.). MS (EI, 70 eV): m/z = 736 [M^+ for $C_8H_4I_2S_2{}^{78}Se^{80}Se_3$]. ^1H NMR (270 MHz, $CDCl_3$): δ = 3.35 (s, 4 H) ppm. IR (neat): $\tilde{\nu}$ = 1088 (m), 1132 (m), 1217 (m), 1223 (m), 1260 (s), 1399 (s), 1416 (m), 1480 (w), 1507 (w) cm^{-1}. $C_8H_4I_2S_2Se_4$ (733.90): calcd. C 13.09, H 0.55; found C 13.16, H 0.50.

2-(4,5-Diiodo-1,3-diselenol-2-ylidene)-5,6-dihydro[1,3]diselenolo[4,5-*b*]-[1,4]diselenine (DIEDSSe): $P(OEt)_3$ (3.0 mL) was added dropwise over a period of 3 min to a refluxing solution of **7**[5] (58 mg, 0.12 mmol) and **1b** (63 mg, 0.15 mmol) in toluene (10 mL), followed by stirring under reflux for 80 min. The same procedure as for DIEDSS was adopted for the separation of the products except for the eluent of the silica-gel column chromatography [CS_2/*n*-hexane (9:1)]. Evaporation of the second orange fraction afforded orange-red crystals of DIEDSSe (22 mg, 21%). M.p. 167 °C (dec.). MS (EI, 70 eV): m/z = 830 [M^+ for $C_8H_4I_2{}^{78}Se_2{}^{80}Se_4$]. ^1H NMR (270 MHz, $CDCl_3$): δ = 3.38 (s, 4 H) ppm. IR (neat): $\tilde{\nu}$ = 1092 (m), 1132 (m), 1223 (m), 1260 (s), 1399 (s), 1416 (m), 1507 (w) cm^{-1}. $C_8H_4I_2Se_6$ (827.69): calcd. C 11.61, H 0.49; found C 11.71, H 0.44.

Crystal Preparation: Single crystals of the salts **8**–**12** were prepared by the electrochemical oxidation (4–6 d) of a CH_2Cl_2 (20 mL) solution containing the corresponding donor molecule (3–6 mg) and $nBu_4NAu(CN)_4$ as a supporting electrolyte (15–39 mg). Platinum electrodes (1.0 mm diameter wire or 1.0×2.0 mm^2 rectangular pillar-shaped) and standard H-shaped cells were employed, and a constant current of 0.5 μA was applied at 20 °C for **8**, **10**–**12** and at 5 °C for **9**. Details of the conditions of Batch A for **11** are as follows: DIETSe (6 mg, 6.8 μmol) and $nBu_4NAu(CN)_4$ (39 mg, 72 μmol) in a standard H-shaped cell were dissolved by CH_2Cl_2 (50 mL) and a small amount of remaining crystals of DIETSe were placed at the side of the anode. Black elongated plate-like crystals (typical size: $0.40 \times 0.06 \times 0.01$ mm^3) grew on the platinum rectangular pillar-shaped electrode under an applied current of 0.5 μA at 20 °C after 5 d.

Crystal Structure Analysis: The diffraction data were collected with a Bruker AXS SMART-APEX CCD system with graphite-monochromated Mo-K_α radiation (λ = 0.71073 Å) (Table 2). Raw frame data were integrated using SAINT[19] and face-indexed absorption corrections[20] were applied. The structures were solved by the direct method (SHELXS-97[21]) and refined by full-matrix least-squares on F^2 with the program package SHELXTL.[22]

CCDC-642673 (for **8**), -642674 (for **9**), -642670 (for **10**), -642671 (for **11**), and -642672 (for **12**) contain the supplementary crystallographic data for this paper. These data can be obtained free of charge from The Cambridge Crystallographic Data Centre via www.ccdc.cam.ac.uk/data_request/cif.

Electronic Band Calculations: Intermolecular overlap integrals were calculated using HOMOs of the donor molecules obtained by the extended Hückel MO calculations using semiempirical parameters for the s and p Slater-type atomic orbitals listed in Table 4. The electronic band dispersions and Fermi surfaces were calculated using the intermolecular overlap integrals under the tight-binding approximation.[16]

Table 4. Semiempirical parameters for Slater-type orbitals.

Orbitals	ζ	I_P/Ryd
I 5s	2.681	–1.713
I 5p	2.322	–0.809
Se 4s	2.44	–1.40
Se 4p	2.07	–0.74
S 3s	2.122	–1.47
S 3p	1.827	–0.79
C 2s	1.625	–1.573
C 2p	1.625	–0.838
H 1s	1.30	–1.0

Electrical Resistivity: The electrical resistivities were measured using the standard four-probe method in the temperature range of 1.6–300 K. Gold wires (10 or 18 μm) were attached to a single crystal using carbon paste, and silver paste was used for wiring the sample to the measurement substrate.

Magnetic Susceptibility: The magnetic properties for **11** were measured with a Quantum Design SQUID magnetometer (MPMS-XL5) for randomly oriented samples operating in the temperature range of 1.8–300 K with a DC magnetic field of 10 Oe or 50 kOe.

The absolute value of molar magnetic susceptibility χ cannot be calculated because of the low applied field of 10 Oe and the discussions of the diamagnetic transition are based on raw data of the magnetization without subtraction of the diamagnetism of the sample holder, DIETSe, and $Au(CN)_4$ anion. The absolute value of χ is obtained by the measurement under the field of 50 kOe. The diamagnetism of the sample holder and DIETSe were obtained from blank experiments under the same conditions as those for the sample measurements. The diamagnetic core susceptibility of the $Au(CN)_4$ anion was evaluated with Pascal's table.

Acknowledgments

This work was partially supported by a Grant-in-Aid for scientific research from the Japan Society for the Promotion of Science (JSPS) and the Ministry of Education, Culture, Sports, Science and Technology (MEXT) (nos. 14740390 and 14204033).

[1] G. R. Desiraju, *Angew. Chem. Int. Ed. Engl.* **1995**, *34*, 2311–2327.

[2] a) T. Imakubo, H. Sawa, R. Kato, *Synth. Met.* **1995**, *73*, 117–122; b) T. Imakubo, H. Sawa, R. Kato, *J. Chem. Soc. Chem. Commun.* **1995**, 1097–1098; c) T. Imakubo, T. Maruyama, H. Sawa, K. Kobayashi, *Chem. Commun.* **1998**, 2021–2022; d) R. Suizu, T. Imakubo, *Org. Biomol. Chem.* **2003**, *1*, 3629–3631; e) K. Hervé, O. Cador, S. Golhen, K. Costuas, J.-F. Halet, T. Shirahata, T. Muto, T. Imakubo, A. Miyazaki, L. Ouahab, *Chem. Mater.* **2006**, *18*, 790–797; f) T. Imakubo, M. Kibune, H. Yoshino, T. Shirahata, K. Yoza, *J. Mater. Chem.* **2006**, *16*, 4110–4116.

[3] a) T. Imakubo, H. Sawa, R. Kato, *J. Chem. Soc. Chem. Commun.* **1995**, 1667–1668; b) T. Imakubo, H. Sawa, R. Kato, *Synth. Met.* **1997**, *86*, 1883–1884; c) T. Imakubo, N. Tajima, M. Tamura, R. Kato, Y. Nishio, K. Kajita, *J. Mater. Chem.* **2002**, *12*, 159–161.

[4] a) T. Imakubo, T. Shirahata, K. Hervé, L. Ouahab, *J. Mater. Chem.* **2006**, *16*, 162–173; b) T. Shirahata, M. Kibune, M. Maesato, T. Kawashima, G. Saito, T. Imakubo, *J. Mater. Chem.* **2006**, *16*, 3381–3390.

[5] T. Imakubo, T. Shirahata, *Chem. Commun.* **2003**, 1940–1941.

[6] T. Shirahata, T. Imakubo, *Org. Biomol. Chem.* **2004**, *2*, 1685–1687.

[7] a) P. Metrangolo, G. Resnati, *Chem. Eur. J.* **2001**, *7*, 2511–2519; b) P. Metrangolo, H. Neukirch, T. Pilati, G. Resnati, *Acc. Chem. Res.* **2005**, *38*, 386–395 and references cited therein.

[8] For other examples of organic conductors based on iodinated TTFs, see: a) R. Gompper, J. Hock, K. Polborn, E. Dormann, H. Winter, *Adv. Mater.* **1995**, *7*, 41–43; b) A. S. Batsanov, A. J. Moore, N. Robertson, A. Green, M. R. Bryce, J. A. K. Howard, A. E. Underhill, *J. Mater. Chem.* **1997**, *7*, 387–389; c) A. S. Batsanov, M. R. Bryce, A. Chesney, J. A. K. Howard, D. E. John, A. J. Moore, C. L. Wood, H. Gershtenman, J. Y. Becker, V. Y. Khodorkovsky, A. Ellern, J. Bernstein, I. F. Perepichka, V. Rotello, M. Grey, A. O. Cuello, *J. Mater. Chem.* **2001**, *11*, 2181–2191; d) B. Domercq, T. Devic, M. Fourmigué, P. Auban-Senzier, E. Canadell, *J. Mater. Chem.* **2001**, *11*, 1570–1575; e) T. Devic, B. Domercq, P. Auban-Senzier, P. Molinié, M. Fourmigué, *Eur. J. Inorg. Chem.* **2002**, 2844–2849; f) J. Nishijo, E. Ogura, J. Yamaura, A. Miyazaki, T. Enoki, T. Takano, Y. Kuwatani, M. Iyoda, *Synth. Met.* **2003**, *133*, 539–541; g) A. Ranganathan, A. El-Ghayoury, C. Mézière, E. Harté, R. Clérac, P. Batail, *Chem. Commun.* **2006**, 2878–2880.

[9] For reviews of organic conductors based on halogenated TTFs, see: a) M. Fourmigué, P. Batail, *Chem. Rev.* **2004**, *104*, 5379–5418; b) T. Imakubo in *TTF Chemistry – Fundamentals and Applications of Tetrathiafulvalene: Halogenated TTFs* (Eds.: J. Yamada, T. Sugimoto), Kodansha & Springer, Tokyo, **2004**, chapter 3 and references cited therein.

[10] For reviews of organic conductors based on selenium analogues of TTFs, see: a) K. Takimiya, T. Otsubo, *Phosphorus Sulfur Silicon Relat. Elem.* **2005**, *180*, 873–881; b) T. Otsubo, K. Takimiya in *TTF Chemistry – Fundamentals and Applications of Tetrathiafulvalene: Selenium Analogues of TTFs* (Eds: J. Yamada, T. Sugimoto), Kodansha & Springer, Tokyo, **2004**, chapter 5 and references cited therein.

[11] V. Y. Lee, E. M. Engler, R. R. Schumaker, S. S. P. Parkin, *J. Chem. Soc. Chem. Commun.* **1983**, 235–236.

[12] A. Morikami, K. Takimiya, Y. Aso, T. Otsubo, *Org. Lett.* **1999**, *1*, 23–25.

[13] For examples of CSe_2-free synthesis of TSeFs see: a) Y. A. Jackson, C. L. White, M. V. Lakshmikantham, M. P. Cava, *Tetrahedron Lett.* **1987**, *28*, 5635–5636; b) G. C. Papavassiliou, S. Y. Yiannopoulos, J. S. Zambounis, K. Kobayashi, K. Umemoto, *Chem. Lett.* **1987**, 1279–1282; c) R. Kato, H. Kobayashi, A. Kobayashi, *Synth. Met.* **1991**, *42*, 2093–2096; d) T. Imakubo, T. Shirahata, M. Kibune, *Chem. Commun.* **2004**, 1590–1591; e) K. Takimiya, H. J. Jeon, T. Otsubo, *Synthesis* **2005**, 2810–2813.

[14] A. Bondi, *J. Phys. Chem.* **1964**, *68*, 411–451.

[15] The LUMOs of the donor molecules, DIEDSS and DIETSe, were calculated by the MNDO-PM3 method using WinMOPAC ver. 3.5 (Fujitsu Ltd.).

[16] T. Mori, A. Kobayashi, Y. Sasaki, H. Kobayashi, G. Saito, H. Inokuchi, *Bull. Chem. Soc. Jpn.* **1984**, *57*, 627–633.

[17] a) M. Munakata, T. Kuroda-Sowa, M. Maekawa, A. Hirota, S. Kitagawa, *Inorg. Chem.* **1995**, *34*, 2705–2710; b) N. Kobayashi, T. Naito, T. Inabe, *Adv. Mater.* **2004**, *16*, 1803–1806.

[18] a) P. J. Nigrey, B. Morosin, E. Duesler, *Synth. Met.* **1988**, *27*, B481–B486; b) N. Svenstrup, J. Becher, *Synthesis* **1995**, 215–235.

[19] *SAINT*, Version 6.45, Bruker AXS, **2003**.

[20] *XPREP*, Bruker AXS, **2003**.

[21] G. M. Sheldrick, *SHELXS97, a program for the solution of crystal structures from X-ray Data*, University Göttingen, Germany, **1997**.

[22] *SHELXTL Reference Manual*, Version 5.03, Siemens Energy & Automation, Inc., Analytical Instrumentation, Madison, WI, USA, **1996**.

Received: May 21, 2007
Published Online: August 29, 2007

